CSIRO PUBLISHING
Soil Research, 2021, **59**, 383–395
https://doi.org/10.1071/SR19317

Spatiotemporal variability of soil organic carbon for different topographic and land use types in a gully watershed on the Chinese Loess Plateau

Fan Yang[A,B,C], *Xiaorong Wei*[A,B], *Mingbin Huang*[A,B,D], *Chenhui Li*[B], *Xiaofang Zhao*[B], and *Zhongdian Zhang*[B]

[A]State Key Laboratory of Soil Erosion and Dryland Farming on the Loess Plateau, Institute of Soil and Water Conservation, Chinese Academy of Sciences and Ministry of Water Resources, Yangling, Shaanxi 712100, China.
[B]Institute of Soil and Water Conservation, Northwest A&F University, Yangling, Shaanxi 712100, China.
[C]University of Chinese Academy of Sciences, Beijing 100049, China.
[D]Corresponding author. Email: hmbd@nwsuaf.edu.cn

Abstract. The ‘Grain-for-Green’ program implemented on the Loess Plateau in China has dramatically changed land use types, and subsequently enhanced the spatiotemporal variability of soil organic carbon (SOC) in the watersheds. However, the spatiotemporal variability of SOC for different topographic and land use types within small watersheds has not been adequately explored following the implementation of the ‘Grain-for-Green’ program. In this study, we determined the spatiotemporal variability of SOC content using the data collected in 1993, 2002, 2005, and 2012 and measured in 2018 and identified its driving factors for different topographic (tableland, sloping land, and gully) and land use types in the Wangdonggou watershed on the Loess Plateau. The spatial patterns of SOC content differed among tableland, sloping land, and gully, with higher spatial variability in gully than sloping land and tableland. The SOC content in the 0–20 cm soil layer in 2018 increased by 8.58%, 26.4%, and 22.2%, compared to 2002, for tableland, sloping land, and gully, respectively. Woodland and grassland had a great potential to sequester and stabilise carbon. The vegetation cover was a relatively dominant factor affecting SOC content throughout the watershed. Our results indicate a close relationship between SOC content and topographic, vegetation, and edaphic variables. This information is critical for understanding SOC dynamics at the watershed scale for sustainable ecological restoration.

Keywords: ecological restoration, land use type, spatial distribution of SOC, temporal change of SOC, topographic type.

Received 4 November 2019, accepted 6 December 2020, published online 29 January 2021

Introduction

Watershed soil organic carbon (SOC) dynamics are linked to nutrient cycling (Zhao *et al*. 2017), sediment transport (Haregeweyn *et al*. 2008; Hancock *et al*. 2019), land use changes (Gelaw *et al*. 2014; Shi *et al*. 2019*a*), and topography (Kunkel *et al*. 2019; Devine *et al*. 2020) and therefore present spatial and temporal variability. A range of studies have investigated the SOC variation in different watersheds. For example, in two watersheds of New South Wales, Australia, SOC concentration was spatially stable for catchments with similar land uses, climate, and geomorphology; and elevation was the most significant control on SOC (Kunkel *et al*. 2019). In the Tiffech watershed of north-east Algeria, the SOC content increased northwards in the area, ranging from 0.53 to 6.9 kg m^{-2}; land use types were demonstrated to have a remarkable impact on SOC distribution (Boubehziz *et al*. 2020). In a karst watershed in south-western China, the mean SOC content was 25.01 g kg^{-1} with a coefficient of variation (CV) of 55.26%, indicating moderate-intensity variation; parent soil material, soil type, land use, slope position, slope direction, and rock exposure rate had significant influences on SOC (Bai and Zhou 2020). Therefore, SOC has a range of spatial patterns, as well as various dominant controlling factors for different watersheds.

Some progress has been made in understanding the long-term temporal changes in SOC at watershed scales. For instance, Wang *et al*. (2011) found that SOC stocks (0–20 cm soil layer) significantly increased from 1998 to 2006 in a small watershed of the Loess Plateau. Wang *et al*. (2012) demonstrated that changes in SOC density (0–20 cm soil layer) occurred in two main phases in replanted cropland in the Chinese hilly Loess Plateau: SOC density slightly increased in the first 10 or 15 years, and then markedly increased. However, revegetation does not always cause soil carbon (C) sequestration and accumulation, which depend on precipitation conditions and vegetation types. If no obvious temporal variations in land use types occur in a catchment, SOC might be temporally stable. Kunkel *et al.* (2019) compared SOC concentrations between 2006 and 2014 in the Krui watershed on the east coast of New South Wales, Australia, and reported that SOC concentrations did not significantly differ over an 8-year period. Nevertheless, studies on long-term monitoring for SOC at large scales are limited because they are labour intensive, time consuming, and expensive.

Both anthropogenic (e.g. land use types and field management) and natural (e.g. climate, soil texture, and topography) factors influence the spatiotemporal variability of SOC in watersheds (Chen *et al.* 2015; Zhao *et al.* 2017; Kunkel *et al.* 2019; Devine *et al.* 2020). Land use changes, characterised as the most substantial human alteration of ecosystems, exert a strong influence on C distribution and stocks by altering the cover and productivity of vegetation as well as physical and chemical characteristics of soil (Fang *et al.* 2012; Deng *et al.* 2014; Oso and Rao 2017; Shi *et al.* 2019*a*). In general, variations in vegetation cover and biomass are accompanied by land use changes. Furthermore, vegetation cover and biomass can affect SOC distribution by influencing the litter input and root distribution in the soil, which in turn influence the soil nutrients as well as microbial community structure and activity (Gunina and Kuzyakov 2014; Lange *et al.* 2015; Deng *et al.* 2018; Yang *et al.* 2018).

Topography, one of the natural factors, is also a key variable affecting SOC spatial distribution (Kunkel *et al.* 2019; Shi *et al.* 2019*b*, 2020; Devine *et al.* 2020). Generally, surface SOC can migrate from the upper slopes and deposit in depressions, especially in heavily eroded regions (Scowcroft *et al.* 2000; Seibert *et al.* 2007). Slope gradient and aspect can control water movement, which contributes to variations in soil characteristics (Tsui *et al.* 2004). Increases in SOC content from the summit and slope to the gully were reported in a Chinese eroded hilly watershed, which indicated prolonged soil erosion and partial deposition towards the gully (Zhu *et al.* 2014). The vegetation biomass as well as the multiple vegetation types on various topographic types can also affect the redistribution of SOC in watersheds (Devine *et al.* 2020). However, recent works mainly focused on the effects of land use changes on spatiotemporal variation of SOC (Poeplau *et al.* 2011; Wang *et al.* 2011; Bae and Ryu 2015) and neglected the potential spatiotemporal differences of SOC for different topographic types as well as the possible redistribution of SOC among different topographic types due to runoff, soil erosion, and deposition at the watershed scale.

The Loess Plateau is known for its deep loess and unique landscapes, but the region has suffered severe soil erosion (Fu 1989; Tang *et al.* 1991; Wang *et al.* 2009) that negatively affects local ecosystems and impedes economic development. A large-scale 'Grain-for-Green' program (GGP) has been implemented in this region by the Chinese Government since 1999, which aimed to decrease soil erosion and restore the ecosystems (Deng *et al.* 2014, 2018; Chen *et al.* 2015). This program has dramatically changed the landscape and almost doubled vegetation coverage from 1999 to 2013 on the Loess Plateau (Chen *et al.* 2015). The fragmented Loess Plateau has various topographic types, including tableland, sloping land, and gullies. The GGP mainly converted farmland on steep slopes to forests and grasslands. Consequently, the obvious land use changes following the GGP implementation have inevitably affected SOC dynamics and changed spatiotemporal variability for different topographic types in watersheds of the Loess Plateau. However, the spatiotemporal variability of SOC content for different topographic types remains unaddressed.

The objectives of this study were to (1) determine the spatial distribution and temporal variation in SOC content for different topographic and land use types in a small watershed after the implementation of GGP and (2) analyse the primary factors impacting the spatiotemporal variability in SOC content for different topographic and land use types. To reach our objectives, the Wangdonggou watershed in the gully region of the Loess Plateau was chosen for this study. The availability of long-term data for climate, land use, and SOC measurements of the Wangdonggou watershed provides unique circumstances for this study.

Materials and methods

Study area

The study was conducted in the Wangdonggou watershed (35°12′–35°16′N, 107°40′–107°42′E) in Changwu County, Shaanxi Province, China (Fig. 1). This small watershed is in a gully region of the Loess Plateau and covers an area of 8.3 km^2, with elevations ranging from 937 to 1239 m. This area is characterised by a continental monsoon climate, with a mean annual temperature of 9.2°C and annual precipitation of 579 mm (averaged from 1960 to 2016), of which more than 58% occurs from July to September (Suo and Huang 2019). The cumulative annual precipitation and annual mean air temperature for the study area from 1993 to 2018 are shown in Fig. 2. The soils in this area have weak cementing forces between the particles and a very low erosion resistance (Li and Su 1991). According to the USDA Soil Taxonomy system (Soil Survey Staff 2014), the soils are classified as Loessi-Orthic Primosols, similar to Cambisols according to the World Reference Base for Soil Resources (IUSS Working Group WRB 2014), and are derived from wind-deposited loess (Wang *et al.* 2017).

In the Wangdonggou watershed, the main topographic types are tableland, sloping land, and gully (Fig. 3), each of which covers approximately one-third of the total study area. The slopes are less than 5° in the tableland, 5–25° in the sloping land, and greater than 25° in the gully (Li and Su 1991). The gully accumulates eroded materials from the tableland and sloping land. The dominant land use types are cropland and orchard on the tableland, and grassland and woodland in the gully (Fig. 1*c*). Sloping land with a slope less than 15° has generally been transformed to terraces. Cropland, apple orchard, grassland, woodland, and abandoned land are the dominant land use types for the sloping land. The cropland in this area is mainly planted with winter wheat (*Triticum aestivum* L.) and spring maize (*Zea mays* L.) (Yao *et al.* 2017). Generally, N (600 kg N ha^{-1}) and P (375 kg P ha^{-1}) fertilisers are applied to cropland every year, with crop residues removed for cooking or feeding cattle (Wang *et al.* 2017). Fertiliser management for apple orchard (*Malus pumila* Mill.) is similar to that for cropland, with no irrigation. Soils are tilled every year to control weeds for better tree

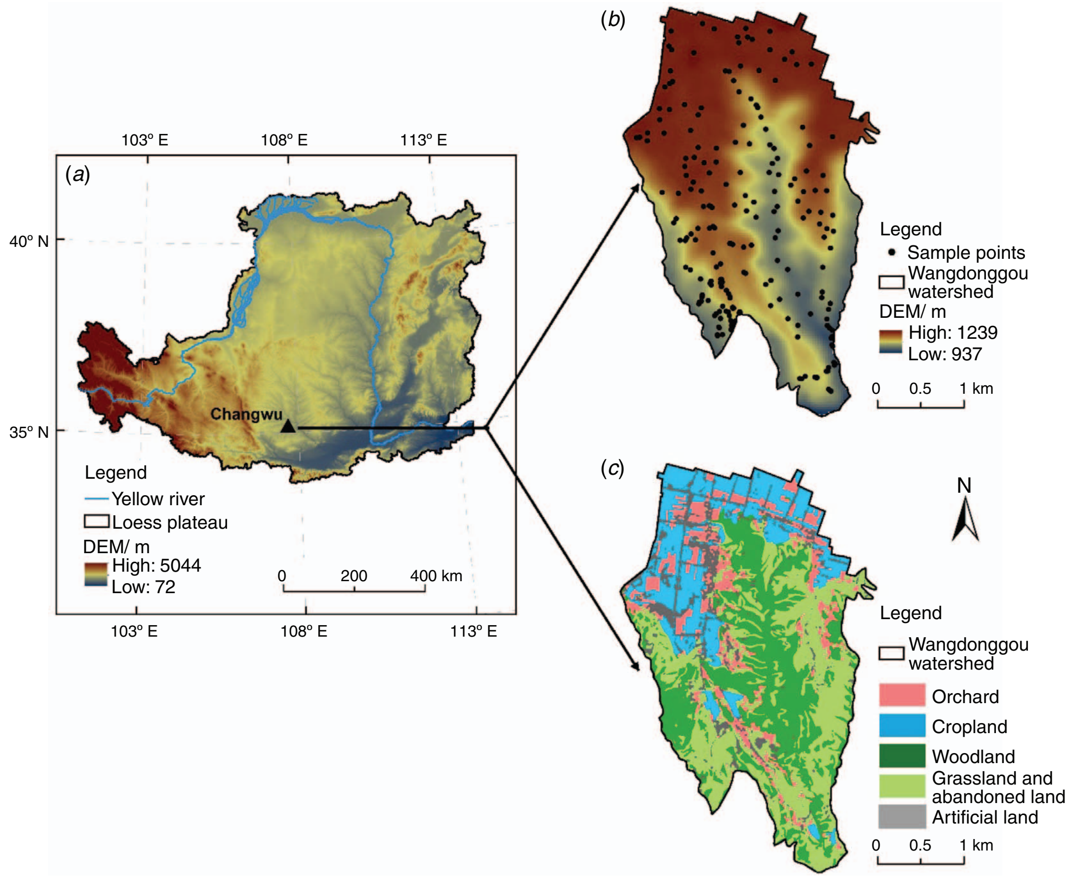

Fig. 1. Location of the (*a*) study area, (*b*) soil sampling locations (2018), and (*c*) land use types in the Wangdonggou watershed.

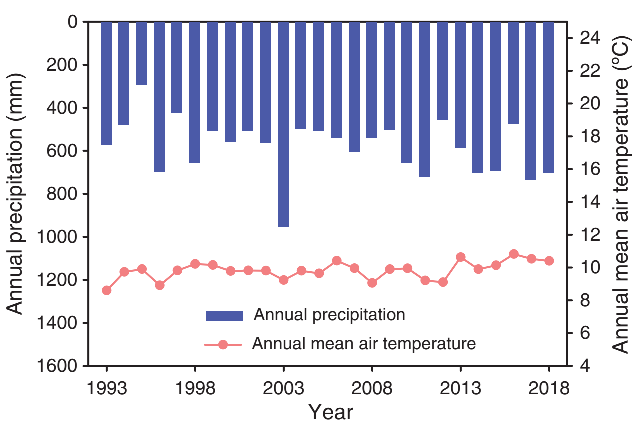

Fig. 2. Cumulative annual precipitation and annual mean air temperature for the study area from 1993 to 2018.

growth. Grassland covered by Russian wormwood (*Artemisia gmelinii*), Old World bluestems (*Bothriochloa ischaemum*) and alfalfa (*Medicago sativa* L.) and woodland covered by black locust (*Robinia pseudoacacia* L.) were regenerated after agricultural abandonment, with anthropogenic perturbation considered less than for cropland and orchard. Abandoned land covered by Russian wormwood and green bristlegrass (*Setaria viridis*) had remained fallow for ~3–15 years, and was generally previously cultivated with winter wheat or spring maize.

Fig. 3. Topographic types in the study watershed. This photo was downloaded from http://cwa.cern.ac.cn/.

Soil sampling and analysis

Soil samples were randomly collected in July 2018 from different topographic types based on the combinations of land use types, slope, aspect, and vegetation cover. A total of 218 sampling locations (~10 m × 10 m) were selected across the whole watershed. The longitude, latitude, and elevations of sampling points were identified with a GPS device. A compass was used to determine the slope and aspect of sampling points. The corresponding land use types, topography, and dominant vegetation species for each sampling point were also recorded while collecting soil samples. The numbers of soil samples for the different topographic types are shown in Table 1.

For each sampling plot (~10 m × 10 m), three to five soil cores were collected using a soil corer (~4 cm in diameter) from two soil layers (0–20 and 20–40 cm) and all replicates were mixed to create one composite sample for each layer. Each of the composite samples was air-dried at room temperature and then passed through a 2-mm sieve for soil particle size analysis and through a 0.25-mm sieve for the SOC analysis.

A prior soil sampling campaign had been conducted in July 2002 in the Wangdonggou watershed. A total of 132 soil samples were collected in the plough layer (0–20 cm) according to their topographic (tableland, sloping land, and gully) and land use (cropland, orchard, grassland, and woodland) types. In each plot, about five soil cores were randomly selected and mixed to form one sample. All soil samples were air-dried and passed through a 0.25-mm sieve for SOC analysis. The laboratory analyses for these samples were done in 2002.

The SOC content was determined using the Walkley–Black dichromate oxidation method (Nelson and Sommers 1982). Soil particle sizes were analysed by laser diffraction using a Mastersizer 2000 (Malvern Instruments, Malvern, England). Soil samples were oven-dried to a constant weight at 105°C and weighed to obtain the gravimetric soil water content (SWC).

Data collection

The Normalized Difference Vegetation Index (NDVI) is defined as a ratio of the difference between near infrared and red reflectance to the sum of near infrared and red reflectance (Tucker 1979). The NDVI is considered as a factor influencing the SOC, and is closely correlated with vegetation cover, biomass, and leaf area index (Xin *et al*. 2016; Zhao *et al*. 2017; Cheng *et al*. 2018). The NDVI has been widely used as a proxy index of vegetation cover for monitoring vegetation restoration (Xin *et al*. 2008, 2016). In our study, NDVI data for the study area were used to manifest the spatial distribution patterns of vegetation cover in the Wangdonggou watershed.

Table 1. Details of soil sampling for different topographic types in the Wangdonggou watershed in 2018

Topographic type	Land use type	Number of soil samples	Sample proportion (%)
Tableland	Cropland	33	15.1
	Orchard	43	19.7
	Grassland	4	1.83
Sloping land	Cropland	15	6.88
	Grassland	26	11.9
	Orchard	6	2.75
	Woodland	48	22.0
	Abandoned land	13	5.96
Gully	Grassland	9	4.13
	Woodland	21	9.63

The land use and NDVI data were obtained from Landsat Enhanced Thematic Mapper (ETM+) images in 2002 and Operational Land Imager (OLI) images in 2018 (30-m resolution) downloaded from the United States Geological Survey (https://earthexplorer.usgs.gov/). The acquisition time of the images was in July of the vegetation growth season to help accurately compare the vegetation conditions. The land use types were identified by support vector machine method. The radiometric calibration and FLAASH atmospheric correction were conducted before calculating the NDVI.

Topographic factors were obtained from a digital elevation model with 30 m × 30 m resolution using ArcGIS 10.5 software (Environmental Systems Research Institute, Redlands, USA). The vector boundary of the Wangdonggou watershed was downloaded from the Loess Plateau Science Data Centre, National Earth System Science Data Sharing Infrastructure, National Science & Technology Infrastructure of China (http://loess.geodata.cn).

The mean SOC contents for the 0–20 cm soil layer for different land uses measured in 1993, 2005, and 2012 and topographic types in 2005 and 2012 in the Wangdonggou watershed were collected from literature to determine any temporal variation in SOC. Relevant sampling information is shown in Table 2. Information about cumulative annual precipitation and annual mean air temperature from 1993 to 2018 was obtained from the meteorological station located at the Wangdonggou watershed. The SOC content in 2002 was only used to conduct spatiotemporal comparisons with that in 2018, and specific analysis for 2002 is not shown. To reduce the potential influence of different sampling locations in 2002 and 2018 on the variation of SOC content, we calculated the mean SOC content using zonal statistics data from the SOC spatial distribution map, produced by regression kriging (RK) interpolation method, to estimate the temporal variation of SOC content for the tableland, sloping land, and gully in both 2002 and 2018.

RK method and its validation

The RK method is a spatial interpolation technique that combines a multiple linear regression (MLR) model with ordinary kriging for the prediction residuals (Hengl *et al*. 2004):

$$\hat{z}(x_0) = \hat{m}(x_0) + \hat{e}(x_0) \tag{1}$$

where $\hat{z}$ is the predicted target variable at the location x_0, $\hat{m}$ is the fitted drift using MLR model, and $\hat{e}$ is the residual that is interpolated using ordinary kriging (Hengl *et al*. 2004; Meng *et al*. 2013).

This method allows the auxiliary variables to interpolate the dependent variables at the un-sampled locations (Hengl *et al*. 2007; Bangroo *et al*. 2020). Given that the topographic and land use types are critical factors influencing the SOC content in our studied watershed, topographic factor and land use type were converted to dummy variables in the MLR model. In order to reduce the variables of land use type, the abandoned

Table 2. Sampling information for the Wangdonggou watershed in 1993, 2005, and 2012
NA, not available

	Year	Soil depth (cm)	Number of soil samples					References
Topographic types			In total	Tableland	Sloping land[A]	Gully		
	2005	0–20	225	NA	NA	NA		Wei *et al*. (2008)
	2012	0–20	259	57	129	73		Wang *et al*. (2017)
Land uses			In total	Cropland	Grassland	Orchard	Woodland	
	1993	0–20	NA	NA	NA	NA	NA	Wang *et al*. (2003)
	2005	0–20	225	NA	NA	NA	NA	Wei *et al*. (2008)
	2012	0–20	259	40	90	48	81	Wang *et al*. (2017)

[A]The data for sloping land are the sum of terrace and sloping land in Wei *et al*. (2008)

land was combined with grassland due to their similar landscape. In addition, altitude, slope, aspect, NDVI, sand content, and clay content were used as independent variables in the MLR model to estimate SOC content.

The total measured samples (218 samples in 2018 and 132 samples in 2002) were divided into two parts: 70% of samples for calibrating the MLR model and 30% of samples for validating the MLR model. The mean estimation error (MEE), mean absolute estimation error (MAEE), and root mean square error (RMSE) were used to evaluate accuracy of the RK method:

$$MEE = \frac{1}{n}\sum_{i=1}^{n}(z_i - \hat{z}_i) \tag{2}$$

$$MAEE = \frac{1}{n}\sum_{i=1}^{n}|z_i - \hat{z}_i| \tag{3}$$

$$RMSE = \sqrt{\frac{1}{n}\sum_{i=1}^{n}(z_i - \hat{z}_i)^2} \tag{4}$$

where n represents the total number of sampling points; z_i and $\hat{z}_i$ are observed and predicted SOC contents at the ith location, respectively.

The s.d. and CVs between measured and predicted SOC contents were used to assess the uncertainty of the RK method in different topographic types.

Statistical analyses

Descriptive statistics and one-sample Kolmogorov–Smirnov (K-S) tests were conducted for SOC content. Logarithmic transformations were used for data that were not normally distributed ($P < 0.05$) for further geostatistical analyses. The Kruskal–Wallis ANOVA test was used to compare differences in SOC content among different land uses and topographic types, whereas a Dunn–Bonferroni test was used for *post hoc* comparisons. Linear regression analyses were carried out to evaluate the relationship between SOC and other edaphic properties (sand, silt, clay, and SWC), topographic variables (altitude, slope, and aspect), and the NDVI. All statistical analyses were performed using SPSS 22.0 for Windows.

The semivariogram was calculated to show the spatial dependence of RK residuals ($\hat{e}$) in 2002 and 2018 using GS$^+$ version 7.0 software. We assessed parameters that can characterise the semivariogram, including nugget variance (C_0), structural variance (C_1), sill (C_0 + C_1), and range (the maximum separation distance over which the spatial dependence of samples is apparent). The coefficient of determination (R^2) and residual sum of squares (RSS) value were used to indicate how well the model semivariogram fitted the experimental semivariogram. Specifically, the model with the highest R^2 and smallest RSS was selected as the best-fitted model. The degree of spatial dependence (GD), which is the ratio of C_0 to $C_0 + C_1$, was used to evaluate the distinct classes of spatial dependence (Gwenzi *et al*. 2011). The GD is strong as the ratio approaches 0, but is weak as this value approaches 1 (Cambardella *et al*. 1994; Castrignanò *et al*. 2011). The residuals were interpolated using ordinary kriging in the Geostatistical module in ArcGIS 10.5 software (Environmental Systems Research Institute) based on the calculated semivariogram parameters.

Results

Characterisation of soil properties

The mean SOC content in the 0–40 cm soil layer of the 2018 samples varied between 4.1 and 10.5, 4.4 and 11.6, and 3.4 and 12.8 g kg^{-1} in the tableland, sloping land, and gully, with CVs of 16.4%, 23.3%, and 25.4%, respectively (Table 3). For all topographic types, soil particle size distribution showed that silt accounted for the largest proportion of the total, followed by clay and sand (Table 3). The CV of the sand was relatively large compared to that for both silt and clay (Table 3). The mean SWC for the gully (17.2%) was higher than that for tableland (16.4%) and sloping land (15.1%) in the 0–40 cm soil layer (Table 3). Over the whole watershed, the mean SOC was 7.2 g kg^{-1} in the 0–40 cm soil layer (Table 3).

Spatial distribution of SOC content

The MLR models for predicting SOC content in 2002 and 2018 are shown in Table 4. The calibration and validation showed that the RK method performed well for estimating the spatial distribution of SOC content in the studied watershed (Table 5). The RMSE varied from 0.63 to 1.41 g kg^{-1} in the calibration and from 0.68 to 1.90 g kg^{-1} in the validation. It is reasonable that the RK method had higher prediction accuracy in the calibration than that in the validation. The prediction accuracy of the RK method also varied in different layers and different topographic types. The values of MAEE

Table 3. Summary statistics for soil properties for different topographic types for the 0–40 cm soil layer in the Wangdonggou watershed in 2018 (n = 218)

CV, coefficient of variation; SOC, soil organic carbon; SWC, soil water content

Topographic type	Soil property	Mean	Min.	Max.	s.e.m.	CV (%)	Skewness	Kurtosis	K-S (P)
Tableland	SOC (g kg^{-1})	6.87	4.12	10.5	0.13	16.4	0.39	0.59	0.20
	Sand (%)	9.34	5.45	14.5	0.24	22.6	0.60	–0.10	0.09
	Silt (%)	64.9	63.0	67.3	0.10	1.41	0.18	–0.23	0.20
	Clay (%)	25.8	21.6	30.6	0.19	6.69	–0.15	0.36	0.20
	SWC (%)	16.4	11.7	20.4	0.19	10.5	0.02	0.06	0.20
Sloping land	SOC (g kg^{-1})	7.11	4.36	11.6	0.16	23.3	0.71	–0.07	0.02
	Sand (%)	11.8	7.49	16.5	0.19	16.6	0.20	–0.22	0.20
	Silt (%)	64.3	61.9	67.0	0.09	1.46	0.22	0.18	0.09
	Clay (%)	23.9	19.6	27.8	0.17	7.48	0.06	–0.25	0.20
	SWC (%)	15.1	9.43	22.6	0.25	17.0	0.42	0.30	0.20
Gully	SOC (g kg^{-1})	8.28	3.41	12.8	0.38	25.4	–0.11	0.01	0.20
	Sand (%)	11.5	5.65	16.3	0.43	20.7	–0.20	0.04	0.20
	Silt (%)	63.1	56.0	65.6	0.32	2.82	–2.12	7.93	0.07
	Clay (%)	25.4	20.7	38.3	0.58	12.6	2.33	8.52	0.01
	SWC (%)	17.2	9.34	22.2	0.59	18.7	–0.43	–0.21	0.20
All areas	SOC (g kg^{-1})	7.19	3.41	12.8	0.11	22.5	0.72	0.47	0.00
	Sand (%)	10.9	5.45	16.5	0.16	21.8	0.08	–0.50	0.20
	Silt (%)	64.3	56.0	67.3	0.08	1.88	–1.54	9.50	0.02
	Clay (%)	24.8	19.6	38.3	0.15	8.90	1.02	5.55	0.20
	SWC (%)	15.9	9.34	22.7	0.17	15.9	0.10	0.09	0.20

Table 4. Multiple linear regression models for predicting SOC content

NDVI, Normalized Difference Vegetation Index; x_1–x_5 are dummy variables; x_1 and x_2 represent topographic types of tableland and gully, respectively; x_3, x_4, and x_5 represent land use types of grassland, woodland, and cropland, respectively; R^2, determination coefficient; P, significance of the regression model

	Soil layer (cm)	Multiple regression equation	R^2	P
2018	0–20	SOC = 8.05 – 0.004 × Aspect + 1.15 × NVDI + 0.20 × Sand – 0.10 × Clay + 0.68x_1 + 1.59x_2 – 0.22x_3 + 1.21x_4	0.38	<0.001
	20–40	SOC = 2.24 – 0.02 × Slope + 0.14 × Sand + 0.07 × Clay + 0.49x_1 – 0.16x_2 – 0.53x_3 – 0.11x_4 – 0.49x_5	0.14	<0.01
2002	0–20	SOC = –2.78 – 0.01 × Aspect + 1.72 × NVDI + 0.47 × Sand + 0.10 × Clay + 1.40x_1 + 1.29x_2 + 0.71x_3 + 1.36x_4	0.50	<0.001

and RMSE were higher in the 0–20 cm than in the 20–40 cm soil layer in 2018. In addition, the absolute values of MEE, MAEE, and RMSE were higher in gully than in tableland and sloping land in the 0–20 cm soil layer in 2002 and 2018.

The parameters of the best-fitted semivariogram models showed that the residuals were spatially structured (Supplementary Table S1). The optimal theoretical variogram models for the MLR residual were exponential and spherical in 0–20 and 20–40 cm soil layers in 2018, respectively. The MLR residual in the two soil layers in 2018 exhibited strong spatial dependence with nuggets representing 2.0–12% of the total variance (Supplementary Table S1). The ranges of spatial dependence for the MLR residual in 0–20 and 20–40 cm soil layers were 369 and 145 m, respectively. By contrast, the best-fitted semivariogram model was spherical for MLR residual in 0–20 cm soil layer in 2002 (Supplementary Table S1). The MLR residual in 2002 was moderately spatially dependent with nugget representing 29% of the total variance.

The SOC prediction map illustrates the spatial variability and distribution of SOC content in the Wangdonggou watershed (Fig. 4). The spatial distribution of SOC content throughout the watershed was patchy. In the 0–20 cm soil layer in both 2002 and 2018, the highest SOC content was mainly distributed alongside the gully, where the dominant land use types were grassland and woodland (Fig. 4*a* and *c*). The higher SOC content in the 20–40 cm soil layer mainly occurred in the north-western tableland in 2018 (Fig. 4*b*).

The topographic and land use types strongly influenced the SOC content (P < 0.05; Figs 5–7). The mean SOC content decreased with increasing soil depth for all topographic and land use types (Figs 5 and 6). The mean SOC content of the topographic types differed between the two soil depths and decreased in the following order: gully (9.88 g kg^{-1}) > sloping land (8.28 g kg^{-1}) > tableland (7.51 g kg^{-1}) in the 0–20 cm soil layer; while in the 20–40 cm soil layer, the highest mean SOC content was in the tableland and the lowest in the sloping land. Additionally, the CVs of SOC content in the two soil layers were the highest in the gully, followed in order by the sloping land and tableland (Fig. 5).

For the tableland, mean SOC content was the highest in orchard, followed by cropland and grassland for the two soil layers (Fig. 7). In the sloping land, the highest mean SOC

Table 5. Prediction accuracy of the regression kriging for estimating the SOC content (g kg^{-1})
MEE, mean estimation error; MAEE, mean absolute estimation error; RMSE, root mean square error

Year	Soil layer (cm)	Topographic types	Calibration MEE	Calibration MAEE	Calibration RMSE	Validation MEE	Validation MAEE	Validation RMSE
2018	0–20	Tableland	0.03	0.67	0.79	–0.05	0.81	1.03
		Sloping land	0.41	0.79	1.04	0.08	0.99	1.22
		Gully	0.78	1.21	1.71	–0.20	1.23	1.83
		All areas	0.32	0.80	1.08	–0.02	0.95	1.27
	20–40	Tableland	0.15	0.55	0.70	0.42	0.70	0.90
		Sloping land	0.00	0.63	0.86	–0.39	0.59	0.68
		Gully	0.05	0.45	0.63	0.13	0.68	0.89
		All areas	0.06	0.57	0.78	0.01	0.65	0.81
2002	0–20	Tableland	–0.19	0.47	0.66	0.03	0.63	0.77
		Sloping land	–0.35	0.92	1.14	–0.64	1.14	1.38
		Gully	0.45	1.10	1.41	0.98	1.60	1.90
		All areas	–0.19	0.74	0.99	–0.12	0.96	1.22

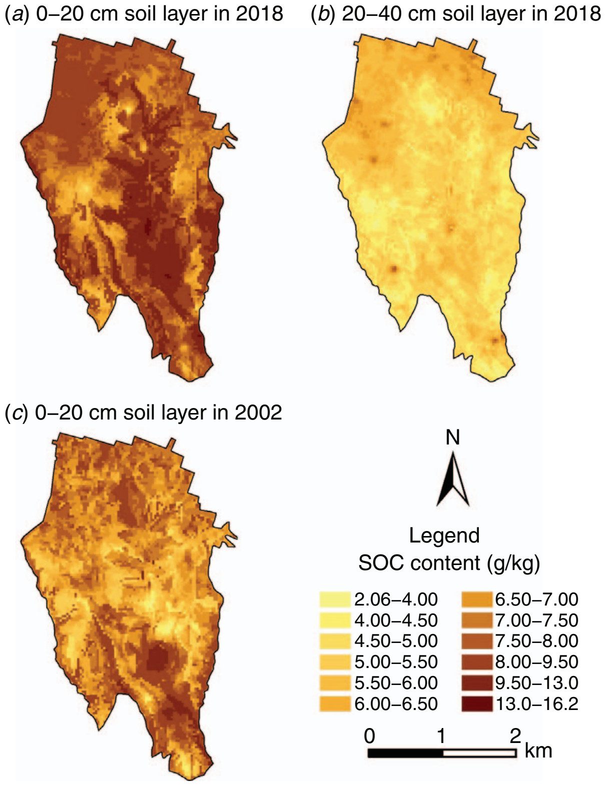

Fig. 4. SOC prediction map for the (*a*) 0–20 and (*b*) 20–40 cm soil layers in 2018, and (*c*) 0–20 cm soil layer in 2002 in the Wangdonggou watershed.

content was in woodland, followed in order by grassland, cropland, orchard, and abandoned land in the 0–20 cm soil layers. In the gully, the mean SOC content in woodland was 1.2 and 1.1 times higher than in grassland in the 0–20 and 20–40 cm soil layers, respectively. In the whole watershed, the mean SOC content was highest in woodland (9.7 g kg^{-1}) in the 0–20 cm soil layer, but was in orchard (5.63 g kg^{-1}) in the 20–40 cm soil layer (Fig. 6). The lowest mean SOC content was in abandoned land for all soil layers among the five land uses (Fig. 6).

Temporal variation of SOC content

The mean SOC content in 2018 increased by 8.58%, 26.4%, and 22.2% in the tableland, sloping land, and gully, respectively, compared with 2002 (Fig. 8*a*). The SOC content declined initially (from 2002 to 2005) and then showed an increasing trend (from 2005 to 2018) in tableland and sloping land (Fig. 8*a*).

In the 0–20 cm soil layer, mean SOC content in 2018 increased by 29.0–66.2% and 8.30–35.9% compared to 1993 and 2002, respectively, for cropland, orchard, grassland, and woodland (Fig. 8*b*). The SOC distribution map shows that the SOC content was significantly higher in 2018 than 2002 (Fig. 4*a* and *c*). As a whole, the SOC content in cropland changed very little and its rate of increase (7.71%) was lower than in orchard (13.4%) in 2018, compared to 1993 (Fig. 8*b*). The SOC content generally increased faster in both woodland and grassland from 1993 to 2012 (except from 2002 to 2005) (Fig. 8*b*).

Linking SOC content to environmental factors

The slope of the linear regression shows the variations in SOC content induced by per unit of change in environmental variables (Table 6). Less remarkable correlations were observed between SOC content and environmental variables in gully versus tableland and sloping land. The sand, clay, SWC, and NDVI were correlated with SOC in the sloping land, but only sand and clay were correlated with SOC in the gully. In tableland, nearly all of the environmental factors (except silt and NDVI) were correlated with SOC content, with per unit changes in NDVI, SWC, and clay inducing greater changes in SOC. For the various land use types, SOC content in the cropland was significantly correlated with altitude, slope, silt, and SWC, with faster changes in SOC content induced by silt and SWC. Significant correlations were noted between the SOC content in orchard with altitude, slope, aspect, sand, clay, and SWC, with the faster changes in SOC content induced by sand and clay. In grassland, SOC content was also significantly correlated with altitude, sand, and SWC. The sand, clay, and NDVI in woodland were significantly correlated with the SOC content. In the whole area, the SOC was significantly

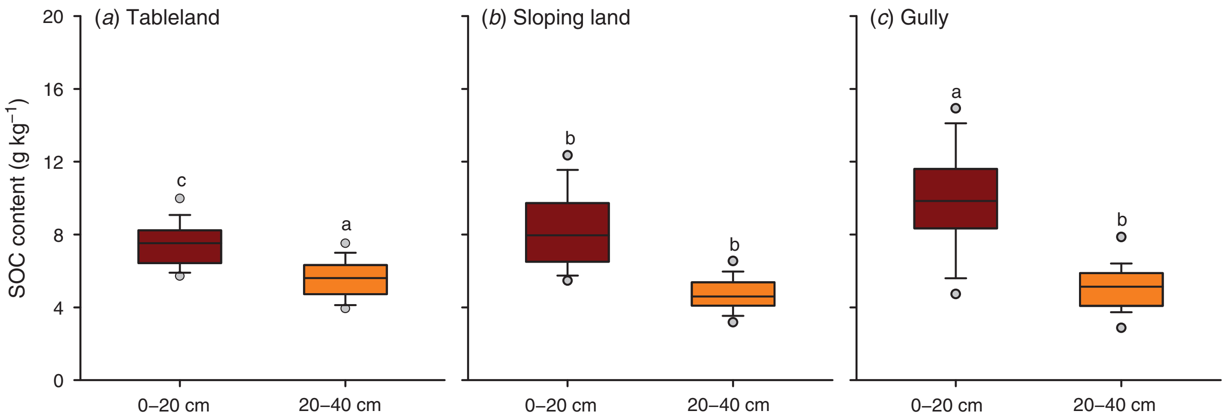

Fig. 5. SOC content for (*a*) tableland, (*b*) sloping land, and (*c*) gully in the Wangdonggou watershed for the 0–20 and 20–40 cm soil layers in 2018. The line in the boxes illustrates the median and the limits of the box are the 25th and 75th percentiles. Whiskers represent nonoutlier ranges. The 5th and 95th percentiles of outliers are shown as circles. Different lowercase letters indicate significant differences in SOC contents among different topographic types in the same soil layer ($P < 0.05$).

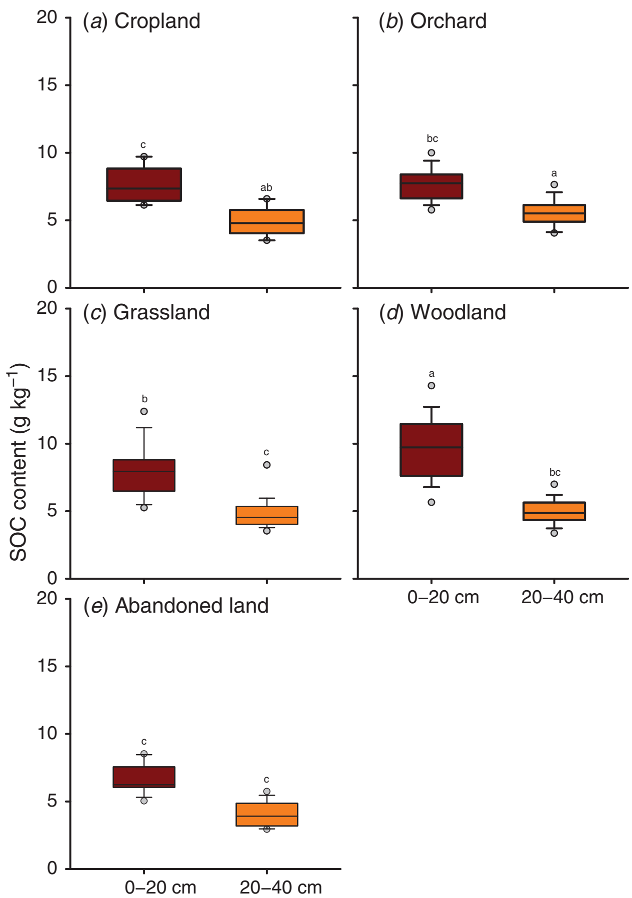

Fig. 6. SOC content for (*a*) cropland, (*b*) orchard, (*c*) grassland, (*d*) woodland, and (*e*) abandoned land in the Wangdonggou watershed for the 0–20 and 20–40 cm soil layers in 2018. The line in the boxes illustrates the median and the limits of the boxes are the 25th and 75th percentiles. Whiskers represent nonoutlier ranges. The 5th and 95th percentiles of outliers are shown as circles. Different lowercase letters indicate significant differences in SOC contents among different land use types in the same soil layer ($P < 0.05$).

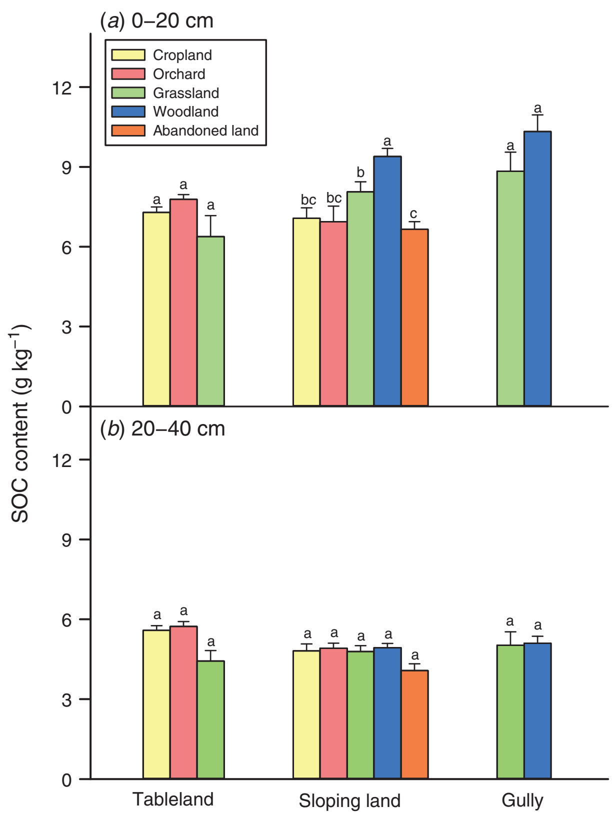

Fig. 7. SOC content for different land uses at topographic type in the Wangdonggou watershed for the (*a*) 0–20 and (*b*) 20–40 cm soil layers in 2018. Values are means + s.e.m. (error bars). Different lowercase letters indicate significant differences in SOC contents among different land use types within the same topographic types of each soil layer ($P < 0.05$).

correlated with aspect, soil particle composition (sand, silt, and clay), SWC, and NDVI, and increased much faster with increasing NDVI.

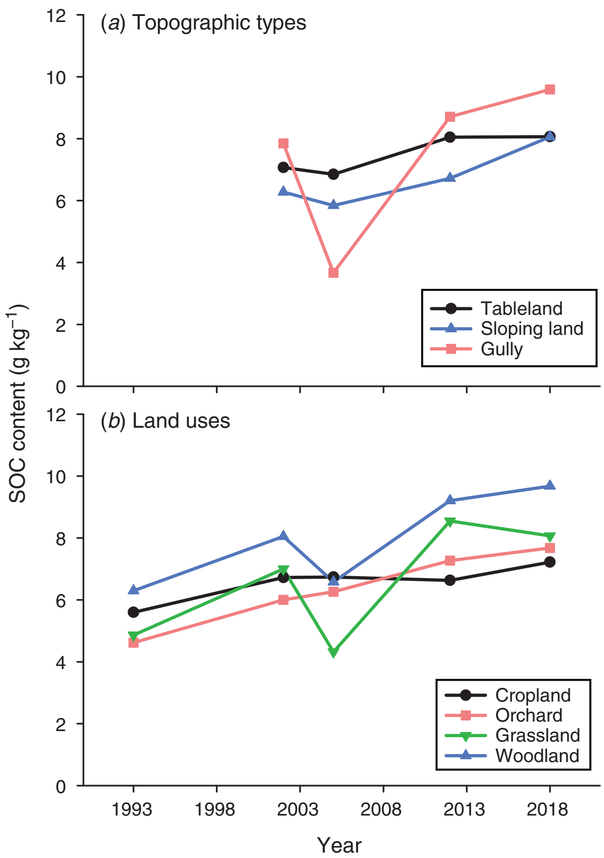

Fig. 8. SOC content for different (*a*) topographic types (from 2002 to 2018) and (*b*) land uses (from 1993 to 2018) in the Wangdonggou watershed for the 0–20 cm soil layer. Data for 1993 are from Wang *et al*. (2003), for 2005 are from Wei *et al*. (2008), and for 2012 are from Wang *et al*. (2017).

Discussion

Spatial distribution of SOC content

The SOC content in the two soil layers (0–20 and 20–40 cm) in 2018 had a high level of spatial variability (Figs 4–7), which was similar to previous studies at the watershed scale (Zhao *et al*. 2017; Cheng *et al*. 2018; Shi *et al*. 2019*a*). One possible explanation could be that the complicated interaction between topography, vegetation coverage, and environmental factors caused the high heterogeneity of SOC in the watershed. The mean values of SOC content in the Wangdonggou watershed decreased from the surface to the lower soil layer, regardless of topographic and land use types (Figs 5–7), which is consistent with previous work (Wang *et al*. 2012, 2017; Deng *et al*. 2018). These results indicate SOC preferentially accumulates at the soil surface. This suggests that, as a C sink, this small watershed is vulnerable.

In general, the highest SOC content for the 0–20 cm soil layer in 2018 mainly occurred alongside the gully of the watershed, where the dominant land use types were grassland and woodland (Fig. 4*a*). The higher SOC content in the gully for the 0–20 cm soil layer is likely connected to complex erosion and deposition process, better vegetation growth, and relatively less human perturbation in the gully of the small watershed (Scowcroft *et al*. 2000; Seibert *et al*. 2007; Zhu *et al*. 2014; Li *et al*. 2017). Specifically, the gully accumulates eroded materials with high SOC content from runoff and soil loss from the tableland and upper slopes (Scowcroft *et al*. 2000; Seibert *et al*. 2007). The annual erosion modulus in the Wangdonggou watershed ranges between 383 and 1869 t km^{-2} (from 1986 to 1999) (Dong *et al*. 2002). Previous work also indicated that soil erosion could account for the changes in SOC and labile C fractions (Cilek 2017; Shi *et al*. 2020). Additionally, more water resources in the gully could provide better conditions for vegetation growth, which in turn could lead to more vegetation litter and root biomass input to the soil (Zhu *et al*. 2014). Indeed, our study observed a mean SWC in the gully (17.2%) that was higher than in tableland (16.4%) and sloping land (15.1%). Furthermore, the decomposition of SOC might be mitigated by the improved water resources (Wang *et al*. 2009) and reduced human disturbance in the gully.

We found that SOC distribution in the 20–40 cm soil layer tended to differ from that observed in the 0–20 cm soil layer in 2018. To be specific, the highest SOC content was mainly in the tableland at 20–40 cm depth, but not in the gully (Fig. 4). The dominant land use types on tableland were cropland and orchard, which had experienced long-term anthropogenic disturbances (e.g. ploughing and fertiliser addition). Therefore, the deeper soil layer in the tableland exhibited relatively high SOC content (Fig. 5), resulting from more organic materials being transported into deeper soil layers, accompanied by artificial tillage and ploughing.

It should be mentioned that the higher MAEE and RMSE values in the 0–20 cm than in the 20–40 cm soil layer indicate that the RK method performed better in the lower soil layer in 2018. The main reason is that SOC spatial variation in the upper soil layer was easily influenced by anthropogenic factors. Furthermore, Table 5 indicates that the RK method had smaller prediction accuracy for estimating SOC content in gully in the 0–20 cm soil layer in 2002 and 2018 due to the more complex terrain in the Wangdonggou watershed.

Topography can induce SOC redistribution, and the land use on topographic types is a key factor affecting SOC content in a watershed. Our study showed that SOC in woodland and grassland was respectively 34.0% and 11.7% higher than in cropland for the 0–20 cm soil layers (Fig. 6). This trend indicates that the restored vegetation greatly contributed to SOC accumulation in the eroded watershed. Similar results were obtained in previous studies (Zhu *et al*. 2014; Han *et al*. 2018). The restored grassland and woodland have larger amounts of aboveground biomass and more abundant roots and, as a result, litter input may be greater and soil erosion can be slowed compared to cropland (Wang *et al*. 2001). Roots and rhizosphere resources exhibit a large and unique habitat which affects microbial abundance and activity and can influence C dynamics (Yang *et al*. 2018). Restoring vegetation can enhance soil aggregation (Tang *et al*. 2010), which provides microenvironments to absorb labile organic matter, and improve the physical protection of SOC from loss and erosion (Zhu *et al*. 2014). In contrast, intensive anthropogenic disturbance (such as tillage management) on

Table 6. Relationships between SOC content and environmental factors for different topographic types and land uses for the 0–40 cm soil layer in the Wangdonggou watershed in 2018

r, correlation coefficient. Asterisks represent significant correlations (*, $P < 0.05$; **, $P < 0.01$). Significant correlation coefficients are shown in bold. SWC, soil water content; NDVI, Normalized Difference Vegetation Index

	Parameter	Altitude	Slope	Aspect	Sand	Silt	Clay	SWC	NDVI
Topographic type									
Tableland	Slope	0.02	0.09	0.00	–0.16	0.17	0.19	0.25	1.37
	Intercept	–16.5	–0.07	7.46	8.33	–4.08	2.07	2.73	6.02
	r	**0.55****	**–0.29****	**–0.24***	**–0.29****	0.14	**0.29***	**0.39****	0.11
Sloping land	Slope	0.00	0.02	0.00	0.43	–0.28	–0.44	0.18	6.05
	Intercept	7.45	6.65	7.55	2.00	25.1	17.7	4.44	3.58
	r	–0.01	0.13	–0.14	**0.51****	–0.16	**–0.48****	**0.27****	**0.38****
Gully	Slope	0.00	–0.12	–0.01	0.30	0.01	0.17	0.14	4.60
	Intercept	11.2	9.60	9.28	0.48	7.70	–0.27	5.87	5.10
	r	–0.09	–0.34	–0.24	**0.54****	0.01	**–0.41***	0.21	0.21
Land use type									
Cropland	Slope	0.01	–0.08	0.00	–0.02	–0.46	0.13	0.15	0.51
	Intercept	–1.17	7.32	6.74	6.82	36.2	3.45	0.29	6.09
	r	**0.35***	**–0.44****	–0.06	–0.03	**–0.32***	0.19	**0.39****	0.05
Orchard	Slope	0.02	–0.09	0.00	–0.39	0.24	0.34	0.31	1.49
	Intercept	–12.4	7.58	7.61	10.3	–8.58	–1.82	1.87	6.04
	r	**0.58****	**–0.43****	**–0.29***	**–0.47****	0.16	**0.40****	**0.56****	0.12
Grassland	Slope	–0.01	–0.07	–0.01	0.31	–0.16	–0.26	0.18	2.49
	Intercept	16.6	8.15	7.79	3.59	17.2	13.5	4.30	5.27
	r	**–0.40***	–0.31	–0.27	**0.34***	–0.09	–0.29	**0.36***	0.14
Woodland	Slope	0.00	0.00	0.00	0.35	–0.22	–0.19	0.09	5.63
	Intercept	8.87	8.05	8.62	3.77	22.2	12.7	6.69	4.28
	r	–0.02	0.02	–0.13	**0.44****	–0.18	**–0.28***	0.13	**0.26***
Abandoned land	Slope	–0.01	–0.05	0.00	0.15	–0.04	–0.17	0.17	1.16
	Intercept	11.0	6.59	5.62	4.12	8.20	9.89	3.10	4.85
	r	–0.17	–0.47	0.10	0.24	–0.04	–0.24	0.39	0.08
All areas									
	Slope	0.00	0.00	0.00	0.21	–0.21	–0.18	0.19	3.89
	Intercept	10.1	7.17	7.71	4.93	20.9	11.5	4.17	4.89
	r	–0.12	0.01	**–0.16***	**0.30****	**–0.16***	**–0.24****	**0.30****	**0.28****

cropland accelerates soil organic matter decomposition (Dolan *et al*. 2006; Cheng *et al*. 2018). Despite the high potential for woodland and grassland to sequester C, SOC content in the sloping land was generally lower than in the gully for the same land use type of each soil layer (Fig. 7). This was due to the severe water and soil erosion that occurred in the sloping land and resulted in SOC loss (Li *et al*. 2017).

Temporal variation of SOC content

Compared with 2002, the SOC content increased in 2018 in the tableland, sloping land, and gully in the 0–20 cm soil layer (Fig. 8*a*). This suggests that vegetation restoration is an effective way to stabilise and sequester C in eroded watershed. The SOC and labile organic C fractions tend to improve after conversion of cropland to grassland, forest, or native vegetation (Smith 2008; Shi *et al*. 2020). Additionally, the increase magnitude of SOC content from 2002 to 2018 in tableland in the 0–20 cm soil layer was less than in the sloping land and gully (Fig. 8*a*). This lower accumulation of SOC content in the tableland might be the result of continuous and intensive disturbance from tillage, ploughing, and weeding on the tableland, regardless of the fertiliser addition to cropland and orchard soils. In general, the increase in SOC content in the soil surface (0–20 cm) in cropland, orchard, grassland, and woodland in 2018, relative to the past 25 years (Fig. 8*b*), suggests that improved SOC accumulation could be attributed to implementation of GGP, a conclusion that agrees with previous studies (Feng *et al*. 2013; Zhao *et al*. 2017). The implementation of GGP caused substantial land use changes and increased the SOC sequestration potential in terrestrial ecosystems on the Loess Plateau (Deng *et al*. 2016). The SOC could be increased by the increase in litter (Deng *et al*. 2018) and organic matter input (Smith 2008), the mitigation of SOC decomposition, and the enhanced SOC stabilisation following vegetation restoration. In addition, the increasing magnitude of SOC content from 1993 to 2018 in orchard was larger than in cropland (Fig. 8*b*). One possible explanation is that, with increasing stand age, the root depth and dry weight density increase, which contribute to greater accumulation of SOC in orchard compared to cropland (Li *et al*. 2019).

The s.d. and CVs for the SOC content were larger in sloping land and gully than in tableland in 2002 and 2018 based on the spatial distribution of SOC content estimated by RK method

(Supplementary Table S2). This indicates that the sloping land and gully had larger uncertainty than tableland when analysing the temporal changes of SOC between 2002 and 2018. The large uncertainty of SOC content in the sloping land and gully may have resulted from the steep slopes and fragmented land, as well as the complicated vegetation cover conditions.

Linking SOC content to environmental factors

The greater changing rate of SOC content was induced by NDVI, soil particle composition, and SWC, than other environmental variables in the Wangdonggou watershed as a whole in 2018 (Table 6), suggesting that these variables might have greater influence on SOC in our study.

Vegetation coverage is considered to be linked to SOC dynamics. The amount of litter inputs in soils as well as the density and distribution of roots varies with vegetation type. These factors can regulate the accumulation, mineralisation, and distribution of SOC and its labile C fractions by altering the soil physical and chemical conditions as well as the microbial community structure and activity (Hanson *et al*. 2000; Gunina and Kuzyakov 2014; Lange *et al*. 2015; Shi *et al*. 2020). Increasing plant coverage is an effective approach to control soil erosion (Zhang *et al*. 2015), which can in turn result in a reduction of C loss. The NDVI is known to be related to vegetation cover, biomass, and leaf area index, and is widely used to assess vegetation restoration (Xin *et al*. 2016). Moreover, a higher NDVI generally indicates a better vegetation cover and canopy density condition. In our study, the NDVI was positively related to SOC content, and the increasing rate of SOC induced by per unit change in NDVI was the highest in the Wangdonggou watershed overall (Tables 4 and 6). This indicates that vegetation cover plays a dominant role in affecting SOC content in this watershed.

Topography (including altitude, slope, and aspect) is characterised as a critical factor affecting the SOC and its spatial distribution in watersheds (Zhu *et al*. 2014; Kunkel *et al*. 2019). Significant correlations between SOC and elevation were observed in large watershed catchments in Krui and Merriwa, Australia (Kunkel *et al*. 2019) and north-eastern India (Choudhury *et al*. 2013). Elevation influences the rainfall distribution, which in turn affects the soil moisture (Xin *et al*. 2016). Soil moisture distribution can further exert influence on vegetation growth and the mineralisation of SOC, which dictates the SOC distribution (Kunkel *et al.* 2019). We found that SOC content was significantly correlated with aspect, but not with altitude and slope, in the Wangdonggou watershed overall (Table 6). The lack of correlation between SOC content and altitude in our study might be because the scale of the altitude in our small watershed is not as great as in other regions. Moreover, anthropogenic activities such as land reclamation and tillage diminish the effects of slope on SOC. The aspect can affect the intensity of surface solar radiation, which influences the distribution of water and heat (Xin *et al*. 2016; Kunkel *et al*. 2019). In general, the southern slopes receive relatively higher radiation and have greater evaporation than the northern slopes, leading to the pronounced difference in vegetation coverage among various aspect slopes.

The SWC is a primary limiting variable for vegetation restoration on the Loess Plateau (Hu *et al*. 2009; Gao *et al*. 2013; Cui *et al*. 2020). Therefore, variations in SWC could result in differences in vegetation growth, soil hydrology, and biochemistry processes. Our study showed that SOC content was significantly correlated with SWC in cropland, orchard, and grassland, as well as the whole watershed (Table 6). Similar interactions between soil water and organic C storage were reported with long-term vegetation restoration on the Loess Plateau, with this interaction weakening with increasing soil depth and restoration stage (Zhang and Shangguan 2016). Owing to the importance of SWC on SOC, future analysis is necessary to fully understand the interactions between SOC and SWC at different spatial scales under ecological restoration.

The SOC content was significantly related to the soil particle composition (Table 6), indicating that the relative amounts of silt, sand, and clay can influence the distribution of SOC content in the Wangdonggou watershed. The soil particle composition can directly affect plant growth as well as sequester C through absorption. In general, land use changes can affect the distribution of soil particle composition because artificial cultivation and perturbation can destroy the soil structure (Han *et al*. 2018). For instance, the improved root biomass after vegetation restoration could impact the bulk density, increase soil aggregation, and eventually contribute to the spatial distribution of SOC (Zhu *et al*. 2014; Deng *et al*. 2018).

Conclusions

Implementation of the GGP program has enhanced SOC accumulation in the 0–20 cm soil layer in the Wangdonggou watershed. Specifically, the SOC content in the 0–20 cm soil layer in the tableland, sloping land, and gully was greater in 2018 than in 2002. The SOC content showed patchy spatial distribution in the watershed and its spatial pattern differed between soil layers in 2018. The topographic and land use type strongly affected the SOC content in this small watershed. Woodland and grassland had the greatest potential to sequester and stabilise C. The vegetation cover was confirmed to play a dominant role in affecting SOC content in the entire Wangdonggou watershed. In summary, vegetation restoration has been an effective approach to create a C sink in this small watershed. Future studies are necessary to conduct long-term monitoring of the quality of soil and vegetation growth after implementation of the GGP to help inform land management strategies and land uses.

Conflicts of interest

The authors declare that they have no conflicts of interest

Acknowledgements

This study was supported by the Strategic Priority Research Program of the Chinese Academy of Sciences (grant no. XDB40020200) and the National Natural Science Foundation of China (grant no. 41571130082). We also thank the editor and three anonymous reviewers for their valuable comments that helped us to greatly improve the manuscript.

References

Bae J, Ryu Y (2015) Land use and land cover changes explain spatial and temporal variations of the soil organic carbon stocks in a constructed urban park. *Landscape and Urban Planning* **136**, 57–67. doi:10.1016/j.landurbplan.2014.11.015

Bai Y, Zhou Y (2020) The main factors controlling spatial variability of soil organic carbon in a small karst watershed, Guizhou Province, China. *Geoderma* **357**, 113938. doi:10.1016/j.geoderma.2019.113938

Bangroo SA, Najar GR, Achin E, Truong PN (2020) Application of predictor variables in spatial quantification of soil organic carbon and total nitrogen using regression kriging in the North Kashmir forest Himalayas. *Catena* **193**, 104632. doi:10.1016/j.catena.2020.104632

Boubehziz S, Khanchoul K, Benslama M, Benslama A, Marchetti A, Francaviglia R, Piccini C (2020) Predictive mapping of soil organic carbon in Northeast Algeria. *Catena* **190**, 104539. doi:10.1016/j.catena.2020.104539

Cambardella CA, Moorman TB, Parkin T, Karlen D, Novak J, Turco R, Konopka A (1994) Field-scale variability of soil properties in central Iowa soils. *Soil Science Society of America Journal* **58**, 1501–1511. doi:10.2136/sssaj1994.03615995005800050033x

Castrignanò A, Buttafuoco G, Comolli R (2011) Using digital elevation model to improve soil pH prediction in an alpine doline. *Pedosphere* **21**, 259–270. doi:10.1016/S1002-0160(11)60126-4

Chen Y, Wang K, Lin Y, Shi W, Song Y, He X (2015) Balancing green and grain trade. *Nature Geoscience* **8**, 739–741. doi:10.1038/ngeo2544

Cheng Y, Li P, Xu G, Li Z, Gao H, Zhao B, Wang T, Wang F, Cheng S (2018) Effects of soil erosion and land use on spatial distribution of soil total phosphorus in a small watershed on the Loess Plateau, China. *Soil & Tillage Research* **184**, 142–152. doi:10.1016/j.still.2018.07.011

Choudhury B, Mohapatra K, Das A, Das PT, Nongkhlaw L, Fiyaz RA, Ngachan S, Hazarika S, Rajkhowa D, Munda G (2013) Spatial variability in distribution of organic carbon stocks in the soils of North East India. *Current Science* **104**, 604–614.

Cilek A (2017) Soil organic carbon losses by water erosion in a Mediterranean watershed. *Soil Research* **55**, 363–375. doi:10.1071/SR16053

Cui Y, Wang X, Zhang X, Ju W, Duan C, Guo X, Wang Y, Fang L (2020) Soil moisture mediates microbial carbon and phosphorus metabolism during vegetation succession in a semiarid region. *Soil Biology & Biochemistry* **147**, 107814. doi:10.1016/j.soilbio.2020.107814

Deng L, Liu GB, Shangguan ZP (2014) Land-use conversion and changing soil carbon stocks in China's 'Grain-for-Green' Program: a synthesis. *Global Change Biology* **20**, 3544–3556. doi:10.1111/gcb.12508

Deng L, Wang K, Tang Z, Shangguan Z (2016) Soil organic carbon dynamics following natural vegetation restoration: Evidence from stable carbon isotopes ($\delta^{13}C$). *Agriculture, Ecosystems & Environment* **221**, 235–244. doi:10.1016/j.agee.2016.01.048

Deng L, Wang K, Zhu G, Liu Y, Chen L, Shangguan Z (2018) Changes of soil carbon in five land use stages following 10 years of vegetation succession on the Loess Plateau, China. *Catena* **171**, 185–192. doi:10.1016/j.catena.2018.07.014

Devine SM, O'Geen AT, Liu H, Jin Y, Dahlke HE, Larsen RE, Dahlgren RA (2020) Terrain attributes and forage productivity predict catchment-scale soil organic carbon stocks. *Geoderma* **368**, 114286. doi:10.1016/j.geoderma.2020.114286

Dolan MS, Clapp CE, Allmaras RR, Baker JM, Molina JAE (2006) Soil organic carbon and nitrogen in a Minnesota soil as related to tillage, residue and nitrogen management. *Soil & Tillage Research* **89**, 221–231. doi:10.1016/j.still.2005.07.015

Dong C, Huang M, Zheng S (2002) Benefit of sediment reduction by biological measures in the watershed scale. *Ying Yong Sheng Tai Xue Bao* **13**, 635–637. [in Chinese with English abstract]

Fang X, Xue Z, Li B, An S (2012) Soil organic carbon distribution in relation to land use and its storage in a small watershed of the Loess Plateau, China. *Catena* **88**, 6–13. doi:10.1016/j.catena.2011.07.012

Feng X, Fu B, Lu N, Zeng Y, Wu B (2013) How ecological restoration alters ecosystem services: an analysis of carbon sequestration in China's Loess Plateau. *Scientific Reports* **3**, 2846. doi:10.1038/srep02846

Fu B (1989) Soil erosion and its control in the loess plateau of China. *Soil Use and Management* **5**, 76–82. doi:10.1111/j.1475-2743.1989.tb00765.x

Gao X, Wu P, Zhao X, Wang J, Shi Y, Zhang B, Tian L, Li H (2013) Estimation of spatial soil moisture averages in a large gully of the Loess Plateau of China through statistical and modeling solutions. *Journal of Hydrology* **486**, 466–478. doi:10.1016/j.jhydrol.2013.02.026

Gelaw AM, Singh BR, Lal R (2014) Soil organic carbon and total nitrogen stocks under different land uses in a semi-arid watershed in Tigray, Northern Ethiopia. *Agriculture, Ecosystems & Environment* **188**, 256–263. doi:10.1016/j.agee.2014.02.035

Gunina A, Kuzyakov Y (2014) Pathways of litter C by formation of aggregates and SOM density fractions: implications from ^{13}C natural abundance. *Soil Biology & Biochemistry* **71**, 95–104. doi:10.1016/j.soilbio.2014.01.011

Gwenzi W, Hinz C, Holmes K, Phillips IR, Mullins IJ (2011) Field-scale spatial variability of saturated hydraulic conductivity on a recently constructed artificial ecosystem. *Geoderma* **166**, 43–56. doi:10.1016/j.geoderma.2011.06.010

Han X, Gao G, Chang R, Li Z, Ma Y, Wang S, Wang C, Lü Y, Fu B (2018) Changes in soil organic and inorganic carbon stocks in deep profiles following cropland abandonment along a precipitation gradient across the Loess Plateau of China. *Agriculture, Ecosystems & Environment* **258**, 1–13. doi:10.1016/j.agee.2018.02.006

Hancock G, Kunkel V, Wells T, Martinez C (2019) Soil organic carbon and soil erosion–Understanding change at the large catchment scale. *Geoderma* **343**, 60–71. doi:10.1016/j.geoderma.2019.02.012

Hanson P, Edwards N, Garten CT, Andrews J (2000) Separating root and soil microbial contributions to soil respiration: a review of methods and observations. *Biogeochemistry* **48**, 115–146. doi:10.1023/A:1006244819642

Haregeweyn N, Poesen J, Deckers J, Nyssen J, Haile M, Govers G, Verstraeten G, Moeyersons J (2008) Sediment-bound nutrient export from micro-dam catchments in Northern Ethiopia. *Land Degradation & Development* **19**, 136–152. doi:10.1002/ldr.830

Hengl T, Heuvelink GBM, Rossiter DG (2007) About regression-kriging: From equations to case studies. *Computers & Geosciences* **33**, 1301–1315. doi:10.1016/j.cageo.2007.05.001

Hengl T, Heuvelink GBM, Stein A (2004) A generic framework for spatial prediction of soil variables based on regression-kriging. *Geoderma* **120**, 75–93. doi:10.1016/j.geoderma.2003.08.018

Hu W, Shao M, Wang Q, Reichardt K (2009) Time stability of soil water storage measured by neutron probe and the effects of calibration procedures in a small watershed. *Catena* **79**, 72–82. doi:10.1016/j.catena.2009.05.012

IUSS Working Group WRB (2014) 'World Reference Base for soil resources 2014: international soil classification system for naming soils and creating legends for soil maps. World Soil Resources Reports No. 106.' (FAO: Rome, Italy)

Kunkel V, Hancock GR, Wells T (2019) Large catchment-scale spatiotemporal distribution of soil organic carbon. *Geoderma* **334**, 175–185. doi:10.1016/j.geoderma.2018.07.046

Lange M, Eisenhauer N, Sierra CA, Bessler H, Engels C, Griffiths RI, Mellado-Vazquez PG, Malik AA, Roy J, Scheu S, Steinbeiss S, Thomson BC, Trumbore SE, Gleixner G (2015) Plant diversity increases soil microbial activity and soil carbon storage. *Nature Communications* **6**, 6707. doi:10.1038/ncomms7707

Li H, Si B, Ma X, Wu P (2019) Deep soil water extraction by apple sequesters organic carbon via root biomass rather than altering soil organic carbon content. *The Science of the Total Environment* **670**, 662–671. doi:10.1016/j.scitotenv.2019.03.267

Li Y, Su S (1991) 'Efficient ecological and economic system in Wangdonggou watershed of Changwu county.' (Scientific and Technical Documents Publishing House Press: Beijing)

Li Z, Nie X, He J, Chang X, Liu C, Liu L, Sun L (2017) Zonal characteristics of sediment-bound organic carbon loss during water erosion: A case study of four typical loess soils in Shaanxi Province. *Catena* **156**, 393–400. doi:10.1016/j.catena.2017.05.001

Meng Q, Liu Z, Borders BE (2013) Assessment of regression kriging for spatial interpolation – comparisons of seven GIS interpolation methods. *Cartography and Geographic Information Science* **40**, 28–39. doi:10.1080/15230406.2013.762138

Nelson DW, Sommers LE (1982) Total carbon, organic carbon and organic matter. In 'Methods of soil analysis, Part 2'. 2nd edn. Agronomy Monograph (Eds AL Page, RH Miller, DR Keeney), vol. 9. pp. 539–579. (ASA and SSSA:, Madison, WI, USA)

Oso V, Rao BKR (2017) Land use conversion in humid tropics influences soil carbon stocks and forms. *Journal of Soil Science and Plant Nutrition* **17**, 543–553. doi:10.4067/S0718-95162017005000039

Poeplau C, Don A, Vesterdal L, Leifeld J, Van Wesemael BAS, Schumacher J, Gensior A (2011) Temporal dynamics of soil organic carbon after land-use change in the temperate zone - carbon response functions as a model approach. *Global Change Biology* **17**, 2415–2427. doi:10.1111/j.1365-2486.2011.02408.x

Scowcroft PG, Turner DR, Vitousek PM (2000) Decomposition of *Metrosideros polymorpha* leaf litter along elevational gradients in Hawaii. *Global Change Biology* **6**, 73–85. doi:10.1046/j.1365-2486.2000.00282.x

Seibert J, Stendahl J, Sørensen R (2007) Topographical influences on soil properties in boreal forests. *Geoderma* **141**, 139–148. doi:10.1016/j.geoderma.2007.05.013

Shi P, Zhang Y, Li P, Li Z, Yu K, Ren Z, Xu G, Cheng S, Wang F, Ma Y (2019*a*) Distribution of soil organic carbon impacted by land-use changes in a hilly watershed of the Loess Plateau, China. *The Science of the Total Environment* **652**, 505–512. doi:10.1016/j.scitotenv.2018.10.172

Shi P, Duan J, Zhang Y, Li P, Wang X, Li Z, Xiao L, Xu G, Lu K, Cheng S (2019*b*) The effects of ecological construction and topography on soil organic carbon and total nitrogen in the Loess Plateau of China. *Environmental Earth Sciences* **78**, 5. doi:10.1007/s12665-018-7992-3

Shi P, Zhang Y, Zhang Y, Yu Y, Li P, Li Z, Xiao L, Xu G, Zhu T (2020) Land-use types and slope topography affect the soil labile carbon fractions in the Loess hilly-gully area of Shaanxi, China. *Archives of Agronomy and Soil Science* **66**, 638–650. doi:10.1080/03650340.2019.1630824

Smith P (2008) Land use change and soil organic carbon dynamics. *Nutrient Cycling in Agroecosystems* **81**, 169–178. doi:10.1007/s10705-007-9138-y

Soil Survey Staff (2014) 'Keys to soil taxonomy.' 12th edn. (United States Department of Agriculture and Natural Resources Conservation Service: Washington, DC, USA)

Suo L, Huang M (2019) Stochastic modelling of soil water dynamics and sustainability for three vegetation types on the Chinese Loess Plateau. *Soil Research* **57**, 500–512. doi:10.1071/SR18118

Tang K, Zhang P, Wang B (1991) Soil erosion and eco-environment changes in Quaternary. *Quaternary Research* **4**, 49–56.

Tang X, Liu S, Liu J, Zhou G (2010) Effects of vegetation restoration and slope positions on soil aggregation and soil carbon accumulation on heavily eroded tropical land of Southern China. *Journal of Soils and Sediments* **10**, 505–513. doi:10.1007/s11368-009-0122-9

Tsui C-C, Chen Z-S, Hsieh C-F (2004) Relationships between soil properties and slope position in a lowland rain forest of southern Taiwan. *Geoderma* **123**, 131–142. doi:10.1016/j.geoderma.2004.01.031

Tucker CJ (1979) Red and photographic infrared linear combinations for monitoring vegetation. *Remote Sensing of Environment* **8**, 127–150. doi:10.1016/0034-4257(79)90013-0

Wang J, Fu B, Qiu Y, Chen L (2001) Soil nutrients in relation to land use and landscape position in the semi-arid small catchment on the loess plateau in China. *Journal of Arid Environments* **48**, 537–550. doi:10.1006/jare.2000.0763

Wang XG, Hao MD, Zhang CX, Wei XR (2003) Study on soil nutrient variation of Wangdonggou small valley. *Research of Soil and Water Conservation* **10**, 81–84. [in Chinese with English abstract]

Wang Y, Fu B, Lü Y, Chen L (2011) Effects of vegetation restoration on soil organic carbon sequestration at multiple scales in semi-arid Loess Plateau, China. *Catena* **85**, 58–66. doi:10.1016/j.catena.2010.12.003

Wang Y, Zhang X, Zhang J, Li S (2009) Spatial Variability of Soil Organic Carbon in a Watershed on the Loess Plateau. *Pedosphere* **19**, 486–495. doi:10.1016/S1002-0160(09)60141-7

Wang Z, Hu Y, Wang R, Guo S, Du L, Zhao M, Yao Z (2017) Soil organic carbon on the fragmented Chinese Loess Plateau: Combining effects of vegetation types and topographic positions. *Soil & Tillage Research* **174**, 1–5. doi:10.1016/j.still.2017.05.005

Wang Z, Liu G-B, Xu M-X, Zhang J, Wang Y, Tang L (2012) Temporal and spatial variations in soil organic carbon sequestration following revegetation in the hilly Loess Plateau, China. *Catena* **99**, 26–33. doi:10.1016/j.catena.2012.07.003

Wei XR, Shao MA, Gao JL (2008) Relationships between soil organic carbon and environmental factors in gully watershed of the Loess Plateau. *Environmental Sciences (Lisse)* **29**, 2879–2884. [in Chinese with English abstract]

Xin Z, Qin Y, Yu X (2016) Spatial variability in soil organic carbon and its influencing factors in a hilly watershed of the Loess Plateau, China. *Catena* **137**, 660–669. doi:10.1016/j.catena.2015.01.028

Xin Z, Xu J, Zheng W (2008) Spatiotemporal variations of vegetation cover on the Chinese Loess Plateau (1981–2006): Impacts of climate changes and human activities. *Science in China. Series D, Earth Sciences* **51**, 67–78. doi:10.1007/s11430-007-0137-2

Yang F, Tian J, Fang H, Gao Y, Zhang X, Yu G, Kuzyakov Y (2018) Spatial heterogeneity of microbial community and enzyme activities in a broad-leaved Korean pine mixed forest. *European Journal of Soil Biology* **88**, 65–72. doi:10.1016/j.ejsobi.2018.07.001

Yao P, Li X, Nan W, Li X, Zhang H, Shen Y, Li S, Yue S (2017) Carbon dioxide fluxes in soil profiles as affected by maize phenology and nitrogen fertilization in the semiarid Loess Plateau. *Agriculture, Ecosystems & Environment* **236**, 120–133. doi:10.1016/j.agee.2016.11.020

Zhang Y, Huang M, Lian J (2015) Spatial distributions of optimal plant coverage for the dominant tree and shrub species along a precipitation gradient on the central Loess Plateau. *Agricultural and Forest Meteorology* **206**, 69–84. doi:10.1016/j.agrformet.2015.03.001

Zhang YW, Shangguan ZP (2016) The coupling interaction of soil water and organic carbon storage in the long vegetation restoration on the Loess Plateau. *Ecological Engineering* **91**, 574–581. doi:10.1016/j.ecoleng.2016.03.033

Zhao B, Li Z, Li P, Xu G, Gao H, Cheng Y, Chang E, Yuan S, Zhang Y, Feng Z (2017) Spatial distribution of soil organic carbon and its influencing factors under the condition of ecological construction in a hilly-gully watershed of the Loess Plateau, China. *Geoderma* **296**, 10–17. doi:10.1016/j.geoderma.2017.02.010

Zhu H, Wu J, Guo S, Huang D, Zhu Q, Ge T, Lei T (2014) Land use and topographic position control soil organic C and N accumulation in eroded hilly watershed of the Loess Plateau. *Catena* **120**, 64–72. doi:10.1016/j.catena.2014.04.007

Handling Editor: Brendan Malone